




Phase-space quantum distributions and information theorySaúl J. C. Salazar ^{*}, Humberto G. Laguna , and Robin P. Sagar *Departamento de Química, Universidad Autónoma Metropolitana, Avenida Ferrocarril San Rafael Atlixco No. 186, Leyes de Reforma 1a Sección, Iztapalapa 09310, Ciudad de México, Mexico*

(Received 28 September 2022; accepted 31 March 2023; published 14 April 2023)

The local structure present in Wigner and Husimi phase-space distributions and their marginals are studied and quantified via information-theoretic quantities. Shannon, Rényi, and cumulative residual entropies of the Wigner and Husimi distributions are examined in the ground and excited states of a harmonic oscillator. The entropies of the Wigner function marginals are lower than the corresponding entropies of the Husimi function marginals, which illustrates how the nodal structure present in the Wigner function is lost upon consideration of the Husimi function. Shannon and cumulative residual entropies of the Wigner function yield entropies which are complex valued. Absolute values and real components of these quantities increase with quantum number, displaying a behavior which is consistent with their real-valued Husimi function counterparts. This comportment is also similar to the real-valued Rényi entropies of the Wigner function. The entropies of the Wigner function are observed to be lower than the corresponding Husimi function ones, in agreement with the results for the marginals. The real components of the Wigner function entropies are seen to be closer to the uncertainty relation bound compared to the corresponding Husimi function entropies. These real components are also closer to the bound when contrasted to the entropic sum of the marginal densities. The Rényi or collision entropy of the Wigner function sits exactly on the bound. Related statistical correlation measures show that the position-momentum correlation is larger in the Wigner function compared to the Husimi function and increases with quantum number.

DOI: [10.1103/PhysRevA.107.042417](https://doi.org/10.1103/PhysRevA.107.042417)**I. INTRODUCTION**

Originally introduced in the study of communication systems, information theory has made an important impact in its application to understanding relevant phenomena in the quantum sciences and beyond. A considerable body of work exists with the application of information-theoretic measures to study quantum systems [1–19]. Among these, Rényi entropies have also been applied to the study of quantum systems [20–26]. However, for the most part, these have been limited to studies in either the position or momentum space representations, via analysis of the respective densities. This is partly due to their connections with the entropic uncertainty relations [27–29]. On the other hand, there are fewer works with regard to the application of information-theoretic measures to phase-space distributions [30–36].

Phase-space or joint position-momentum distributions have been examined in quantum mechanics. The connections between quantum mechanics and statistical mechanics, when seeking quantum corrections to thermodynamics, was addressed by Wigner [37] in his foundational paper of phase-space representations. The Wigner function provides such a connection, but has the characteristic of not being positive definite, giving rise to fundamental questions about the uncertainty principle and its connection with the phase-space description. Later on, the Wigner function was shown to be the solution of the quantum analog of the Liouville equa-

tion [38,39]. This has led to its application and study in fields such as quantum thermodynamics [40,41].

Attempts to address the negativity of the Wigner function have also been made. It has been shown that an infinite number of phase-space distribution functions can be generated using parametric families of functions [42–44]. Nevertheless, the Wigner function is the only one that is bilinear in the wave function and with the correct marginals [45]. The Wigner function marginals are indeed the position and momentum space densities.

However, applying a Gaussian convolution to the Wigner function yields the Husimi function [44,46]. This is equivalent to applying a Gaussian filter to a distribution. Hence, if the Wigner function is experimentally accessible [47–52], the Husimi function can also be obtained. The Husimi function has the advantage that it is a positive-definite function, but does not give the position and momentum space densities as its marginals.

The aim of this work is an examination and assessment of Shannon, Rényi, and cumulative residual entropies as applied to the Wigner and Husimi functions and their marginals. Related statistical correlation measures, which quantify the position-momentum correlation, are also discussed. The harmonic oscillator is studied, since its ground-state Wigner function provides the floor of the bound, in the formulations of the Heisenberg uncertainty principle. One goal will be to examine these bounds, given in terms of Wigner and Husimi function entropies, in excited states. Our focus here is to evaluate different expressions for entropies and mutual information of the Wigner and Husimi functions and to assess

^{*}sjcsalazar@xanum.uam.mx

their consistency with regard to interpretations. Definitions are provided in the following before moving on to the discussion and presentation of results.

II. WIGNER FUNCTION AND SHANNON ENTROPIES

The Wigner distribution or Wigner function (WF) is defined in terms of the Weyl transform as

$$W(x, p) = \frac{1}{\pi\hbar} \int \rho(x-y, x+y) e^{-2ipy/\hbar} dy, \quad (1)$$

where $\rho(x-y, x+y)$ is the density matrix. For a pure state, where the density matrix is given in terms of the wave function $\rho(x-y, x+y) = \Psi^*(x-y)\Psi(x+y)$, the WF is

$$W(x, p) = \frac{1}{\pi\hbar} \int \Psi^*(x-y)\Psi(x+y) e^{-2ipy/\hbar} dy. \quad (2)$$

The limits on all integrals are $[-\infty, \infty]$ unless stated otherwise.

One of the strengths of the formulation in terms of Wigner functions is that its marginals are the position and momentum space densities of the system

$$\rho(x) = \int W(x, p) dp, \quad (3)$$

$$\pi(p) = \int W(x, p) dx, \quad (4)$$

respectively. Here $\rho(x)$ and $\pi(p)$ are normalized to unity, thus satisfying

$$\iint W(x, p) dx dp = 1. \quad (5)$$

The marginal densities are positive definite, while the parent distribution (WF) is not necessarily so. The WF is commonly referred to as a quasiprobability distribution since it can possess negative regions. These negative regions and their volumes are indeed a manifestation of quantum effects, which makes their study interesting [53]. Note that in spite of the negative regions, the WF is a properly normalizable function, a requisite for its interpretation as a probability density. It is the negative regions which present issues in the definition of corresponding information-theoretic quantities [54]. For example, the Shannon entropy of the Wigner function [32] is defined as

$$S_W = - \iint W(x, p) \ln[W(x, p)] dx dp. \quad (6)$$

However, since the WF possesses negative regions, its corresponding Shannon entropy is not real valued and has imaginary components. The magnitude of the imaginary component is related to the volume of the negative regions. The real component also has contributions from these negative parts [32].

On the other hand, the Shannon entropies of the marginals of the WF are defined as

$$S_W^x = S_x = - \int \rho(x) \ln[\rho(x)] dx, \quad (7)$$

$$S_W^p = S_p = - \int \pi(p) \ln[\pi(p)] dp \quad (8)$$

and are real valued due to the positivity of the position and momentum space densities. The entropies of the marginals quantify the entropic uncertainty relation.

III. HUSIMI FUNCTION AND SHANNON ENTROPIES

The Husimi function (HF) can be obtained by the Weierstrass transform applied to the Wigner function [46,55–57]

$$H(x, p) = \frac{1}{\pi\hbar} \iint W(x, p) e^{-(x-x')^2/2s^2} e^{-(p-p')^2 2s^2/\hbar^2} dx' dp'. \quad (9)$$

The s parameter is arbitrary, with each distinct election producing a different set of basis functions $\{|x, p\rangle\}$ [58]. As $s \rightarrow 0$, one recovers the position space density, while for $s \rightarrow \infty$, one gets the momentum space density. In this work, the value of s is set at unity.

The HF is positive definite and avoids the negativity of the WF. However, the HF does not have the same local structure as the WF since it has been passed through a Gaussian filter. One of the goals of this work is to examine and quantify the differences between the local behaviors of the WF and HFs and their marginals. The HF marginals

$$\rho_H(x) = \int H(x, p) dp, \quad (10)$$

$$\pi_H(p) = \int H(x, p) dx \quad (11)$$

are not the position and momentum space densities. Here $\rho_H(x)$ and $\pi_H(p)$ are normalized to unity, thus satisfying

$$\iint H(x, p) dx dp = 1. \quad (12)$$

The Shannon entropy of the Husimi function, known as the Wehrl entropy [30], is

$$S_H = - \iint H(x, p) \ln[H(x, p)] dx dp. \quad (13)$$

Since the HF is positive definite, its Shannon entropy is real valued. The entropies of the marginals of the HF are

$$S_H^x = - \int \rho_H(x) \ln[\rho_H(x)] dx, \quad (14)$$

$$S_H^p = - \int \pi_H(p) \ln[\pi_H(p)] dp. \quad (15)$$

There is one further definition which merits attention. A relative (Kullback-Leibler) entropy is a measure of the distance between two distributions. For example, this can be defined in terms of the position space WF and HF marginals as

$$S_{KL} = \int \rho(x) \ln \left(\frac{\rho(x)}{\rho_H(x)} \right) dx \quad (16)$$

and gives a measure of the distance or similarity between the position space density and the HF marginal. This measure is well defined when the densities share the same zero values (nodal structure) or when the density in the denominator does not exhibit zeros.

IV. MUTUAL INFORMATION

There is also current interest in the mutual information, a measure of the statistical correlation between two or more variables. The position-momentum statistical correlation in the WF may be defined as

$$I_W = \iint W(x, p) \ln \left(\frac{W(x, p)}{\rho(x)\pi(p)} \right) dx dp$$

$$= S_W^x + S_W^p - S_W = S_t - S_W \tag{17}$$

and can be interpreted as a relative entropy or distance between the WF and a reference phase-space distribution, which is separable and a product of the marginal distributions. This quantity is also complex valued due to S_W . Moreover, the strength of such a proposal lies in the recognition that this correlation between variables is in terms of the difference from a quantity S_t that has been used to quantify the entropic uncertainty relationship [27,28]

$$S_t = S_W^x + S_W^p \geq 1 + \ln \pi. \tag{18}$$

There is also a similar relationship for the HF [31,35]

$$S_t(H) = S_H^x + S_H^p \geq S_H \geq 1 + \ln 2\pi. \tag{19}$$

Note the presence of S_H in Eq. (19), while Eq. (18) for S_t is not formulated in terms of S_W since it is complex valued. One avenue of this work will be to explore how the real component of S_W behaves with regard to S_t and to the bound in Eq. (18) in excited states. This is appealing since the WF and HF of the ground-state harmonic oscillator provide the floor of the respective bounds given in Eqs. (18) and (19). Likewise, one can also define the mutual information for the HF [35]

$$I_H = \iint H(x, p) \ln \left(\frac{H(x, p)}{\rho_H(x)\pi_H(p)} \right) dx dp$$

$$= S_H^x + S_H^p - S_H \geq 0. \tag{20}$$

A further aim of this work is to compare the behavior of I_W and I_H in the harmonic oscillator to discuss similarities or differences.

V. CUMULATIVE DISTRIBUTIONS

Another avenue to tackling the negativity of the WF lies in the use of related cumulative or survival distributions. The survival s distribution of the WF is

$$s_W(a, b) = \int_a^\infty \int_b^\infty W(x, p) dx dp, \tag{21}$$

while the survivals of the marginals are

$$s_W^x(a) = \int_a^\infty \rho(x) dx, \tag{22}$$

$$s_W^p(b) = \int_b^\infty \pi(p) dp. \tag{23}$$

The idea is that integration over regions of the WF could result in the disappearance of the negative regions and translate into the appearance of structure.

The cumulative residual entropy C [59] is defined for the marginals as

$$C_W^x = - \int s_W^x(a) \ln s_W^x(a) da, \tag{24}$$

$$C_W^p = - \int s_W^p(b) \ln s_W^p(b) db. \tag{25}$$

An uncertainty relationship in terms of these cumulative entropies can be provided if one takes the $n = 0$ harmonic-oscillator state as the saturation point for the bound,

$$S_t(C_W) = C_W^x + C_W^p \geq c_1 = - \int \text{erfc}(a) \ln \left(\frac{\text{erfc}(a)}{2} \right) da, \tag{26}$$

where $\text{erfc}(a)$ is the complementary error function and $\frac{\text{erfc}(a)}{2}$ is the survival density of the $n = 0$ oscillator state.

There is also a cumulative residual Jeffreys divergence R [60] which can be used to measure the distance between the WF and HF survival densities of the marginals,

$$R = \int s_W^x(a) \ln \left(\frac{s_W^x(a)}{s_H^x(a)} \right) da + \int s_H^x(a) \ln \left(\frac{s_H^x(a)}{s_W^x(a)} \right) da. \tag{27}$$

This is the symmetrized survival counterpart to the relative entropy of the parent distributions given in Eq. (16).

Application of a similar entropic definition to the two-variable WF survival distribution in Eq. (21) results in divergence of the required integral. Thus, entropic-type definitions for two-variable distributions have been obtained [59] from use of conditional entropies. The joint cumulative residual entropy J is defined for the WF as

$$J_W = C_W^x + E[\epsilon(b|x)], \tag{28}$$

where

$$E[\epsilon(b|x)] = - \iint P(x, p > b) \ln \left(\frac{P(x, p > b)}{\rho(x)} \right) db dx, \tag{29}$$

with

$$P(x, p > b) = \int_b^\infty W(x, p) dp \tag{30}$$

an auxiliary density.

The counterpart to the mutual information is the cross cumulative residual entropy \mathcal{C} [59], which measures the correlation in a survival distribution. It is defined for the WF as

$$\mathcal{C}_W = C_W^x - E[\epsilon(b|x)]. \tag{31}$$

It is also possible to define J and \mathcal{C} using momentum space quantities C_W^p and $E[\epsilon(b|p)]$.

The corresponding information measures for the HF are defined in exactly the same manner as the ones for the WF, by substituting the HF densities for the WF ones in the expressions above. These are not provided for brevity. The uncertainty relation for the marginals of the HF is

$$S_t(C_H) = C_H^x + C_H^p \geq c_2 = - \frac{1}{\sqrt{2}} \int \text{erfc}(a) \ln \left(\frac{\text{erfc}(a)}{2\sqrt{2}} \right) da, \tag{32}$$

where $\frac{\text{erfc}(a)}{2\sqrt{2}}$ is the survival density of the Husimi marginals for the $n = 0$ state.

VI. RÉNYI ENTROPY AND INFORMATION

Thus far, we have discussed options for obtaining densities that are related to the WF, which are positive definite. Such densities are attractive since there are no issues relating to their use in entropic definitions. Densities which are not positive definite (such as the WF) yield complex-valued entropies. Another path forward is to use the nonpositive-definite densities, but in entropic expressions which do not yield complex-valued quantities.

The Rényi entropies are parameter dependent and are given for the WF marginals as

$$\begin{aligned} R_\alpha^x &= \frac{1}{1-\alpha} \ln \left(\int \rho(x)^\alpha dx \right), \\ R_\beta^p &= \frac{1}{1-\beta} \ln \left(\int \pi(p)^\beta dp \right). \end{aligned} \quad (33)$$

The Shannon entropies are recovered in the limit

$$\lim_{\alpha \rightarrow 1} R_\alpha^x = S_W^x, \quad \lim_{\beta \rightarrow 1} R_\beta^p = S_W^p. \quad (34)$$

We now consider the Rényi entropy of the WF. In the following, the same label (α) is used for the parameter as in the position space entropy. The reasoning for this election will be apparent in the subsequent discussion. The particular choice of $\alpha = 2$ is known as the collision entropy and in the context of the WF is

$$R_2^W = -\ln \left(\iint W(x, p)^2 dx dp \right). \quad (35)$$

Note that even though the WF has negative regions, the integrand above is positive valued due to the particular choice of $\alpha = 2$. The state overlap in the WF is defined as [61]

$$|\langle \psi | \theta \rangle|^2 = 2\pi \hbar \iint W_\psi(x, p) W_\theta(x, p) dx dp. \quad (36)$$

With $\psi = \theta$, the left-hand side of Eq. (36) is unity, which yields the collision entropy as ($\hbar = 1$)

$$R_2^W = \ln(2\pi). \quad (37)$$

Here R_2^W is real valued and a constant, independent of the particular state.

Entropic uncertainty relations in terms of Rényi entropies of the marginals have been given as [62,63]

$$R_\beta^p + R_\alpha^x \geq -\frac{1}{2(1-\beta)} \ln \left(\frac{\beta}{\pi} \right) - \frac{1}{2(1-\alpha)} \ln \left(\frac{\alpha}{\pi} \right), \quad (38)$$

with the restriction that $\frac{1}{\alpha} + \frac{1}{\beta} = 2$. The use of such a relation with different values of the parameter in each space presents an obstacle to the comparison of the marginal entropies with that of a suitably defined phase-space entropy. Which of the two values would one consider for the phase-space entropy? Thus, for an adequate comparison, one would need to use the same parameter value for each entropic definition. Moreover, this parameter should be even valued to yield a real-valued phase-space Rényi entropy.

The Shannon entropic uncertainty relationship saturates for a Gaussian distribution ($n = 0$ oscillator). We proceed by using this to write a Rényi uncertainty relation for $\alpha = \beta = 2, 4$ as

$$\begin{aligned} S_i(R_2^W) &= R_2^p + R_2^x \geq \ln 2\pi, \\ S_i(R_4^W) &= R_4^p + R_4^x \geq \ln \sqrt[3]{4\pi}, \end{aligned} \quad (39)$$

where the expressions on the right-hand side correspond to the Rényi entropies of the marginals for the $n = 0$ state. Another goal of this work is to examine these bounds, given in terms of the Rényi entropies of the marginals, and to compare them to R_2^W and R_4^W . These phase-space entropies are real valued and one can conjecture as to their presence in the equation above.

The Rényi divergence in position space is defined as

$$D_R = \frac{1}{\alpha - 1} \ln \left(\int \frac{\rho(x)^\alpha}{\rho_H(x)^{\alpha-1}} dx \right) \quad (40)$$

and is a measure of the distance between the two densities $\rho(x)$ and $\rho_H(x)$. A Rényi mutual information with $\alpha = 2$ is defined for the WF as

$$I_R^W = \ln \left(\iint \frac{W(x, p)^2}{\pi(p)\rho(x)} dx dp \right). \quad (41)$$

The integral diverges when $\pi(p)$ or $\rho(x)$ in the denominator of the expression presents zeros (nodal structure) that are not shared with the WF in the numerator. On the other hand, the measure is finite valued when applied to the HF and its marginals.

The one-variable Cauchy-Schwarz divergence [64] has a form similar to I_R^W . It is defined, in general, in terms of $f(x)$ and $g(x)$, as

$$D_{CS} = -\ln \left(\frac{\int [f(x)g(x)]^2 dx}{\sqrt{[\int f(x)^2 dx][\int g(x)^2 dx]}} \right). \quad (42)$$

This allows us to define the Cauchy-Schwarz mutual information [65] in terms of the WF, replacing $f(x)$ with $W(x, p)$, $g(x)$ with $\rho(x)\pi(p)$, and dx with $dx dp$, in Eq. (42), as

$$\begin{aligned} I_W^{CS} &= R_2(W(x, p) \times \pi(p)\rho(x)) - \frac{1}{2}R_2(W(x, p)) \\ &\quad - \frac{1}{2}R_2(\pi(p)\rho(x)). \end{aligned} \quad (43)$$

Corresponding measures for the HF (R_2^H , I_R^H , and I_H^{CS}) are obtained by substituting the HF for the WF and replacing the marginals $\rho(x)$ and $\pi(p)$ by $\rho_H(x)$ and $\pi_H(p)$ in the expressions above. The uncertainty relations in terms of the Husimi marginals are

$$\begin{aligned} S_i(R_2^H) &= R_2^p(H) + R_2^x(H) \geq \ln 4\pi, \\ S_i(R_4^H) &= R_4^p(H) + R_4^x(H) \geq \ln 2\sqrt[3]{4\pi} \end{aligned} \quad (44)$$

for $\alpha = \beta = 2, 4$. Again, one can conjecture the presence of R_2^H and R_4^H in these relations.

VII. HARMONIC OSCILLATOR

We now focus our attention on the harmonic oscillator in this work. Our goal is to compare and contrast the entropic and correlation measures as a function of quantum number n . Such

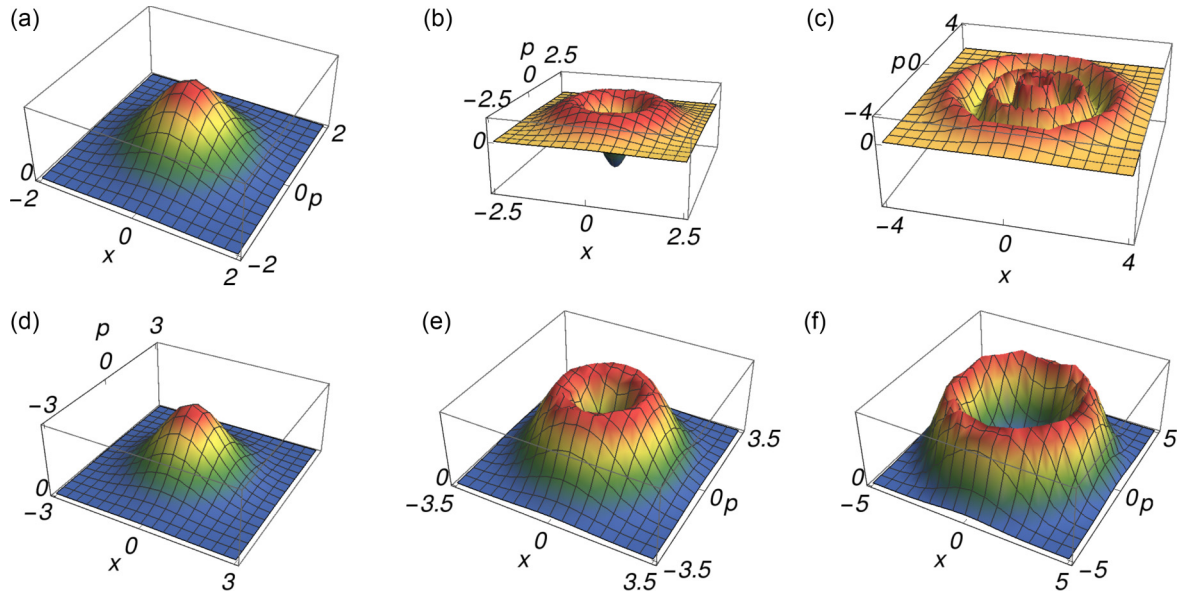


FIG. 1. Plots of (a)–(c) the Wigner function $W(x, p)$ and (d)–(f) the Husimi function $H(x, p)$, with the oscillator frequency $\omega = 1$, for states (a) and (d) $n = 0$, (b) and (e) $n = 1$, and (c) and (f) $n = 5$. The value of ω is set at unity in all subsequent plots. Densities are given in atomic units.

an analysis should provide insights into the similarities or differences between the phase-space distributions of ground and excited states and the characteristics of these distributions upon excitation.

The WF of a harmonic oscillator with quantum number n is

$$W_n(x, p) = (\pi \hbar)^{-1} (-1)^n e^{-2\mathcal{H}/\hbar\omega} L_n\left(\frac{4\mathcal{H}}{\hbar\omega}\right), \quad (45)$$

where \mathcal{H} is the Hamiltonian

$$\mathcal{H}(x, p) = \frac{p^2}{2m} + \frac{m\omega^2 x^2}{2}. \quad (46)$$

Here $L_n(z)$ is the n th-order Laguerre polynomial and ω is the oscillator frequency.

The HF of the oscillator is

$$H_n(x, p) = (2\pi \hbar n!)^{-1} e^{-\mathcal{H}/\hbar\omega} \left(\frac{\mathcal{H}}{\hbar\omega}\right)^n. \quad (47)$$

We restrict our consideration to the case of $\omega = 1$ and use units of $\hbar = m = 1$. The choice of ω simplifies the analysis, since $\rho(x) = \pi(p)$ and $\rho_H(x) = \pi_H(p)$.

In particular, we compare the behavior of the Shannon entropies of the Wigner and Husimi functions. The Shannon (Wehrl) entropy of the Husimi function is real valued, while the Shannon entropy of the Wigner function is complex valued. The behavior of the Shannon entropies of the Husimi function is used as a guide to evaluate the behavior of the real and imaginary components of the Wigner function entropy. The entropies of the respective marginals are also considered. One would expect that the Shannon entropies of the Husimi function would be greater than the corresponding ones for the Wigner function; however, their quantification is important in the calculation of statistical correlation (mutual information) measures, where the correlation between the x and p variables is measured. Entropic sums of the Wigner and Husimi

function marginals, which form the basis of entropic uncertainty relations, will also be compared to the entropies of their parent distributions. Furthermore, other classes of entropies, such as the Rényi and cumulative residual entropies, are explored from the perspective of obtaining real-valued Wigner entropies and correlation measures. Comparisons among the behaviors of the measures are performed as an aid in evaluating the consistency of the results obtained from the different measures, which is an important consideration in any related interpretations.

VIII. RESULTS AND DISCUSSION

We begin the discussion by considering the local structure present in the WF and HF, their cumulative distributions, and respective marginal densities. It is this structure which is quantified by the information-theoretic measures. We then proceed to examine the behaviors of the entropic and correlation measures in subsequent sections.

A. Density functions

Figure 1 presents the WF and HF for different states of the harmonic oscillator. The WF and HF are similar in appearance in the ground state. One can appreciate the appearance of a nodal structure in both cases as n is increased. However, the differences are more apparent for larger n . The nodal structure is more visible in the WF with $n = 5$ as compared to the HF. Furthermore, the chosen perspective illustrates the negative regions of the WF for $n = 1, 5$, which are not present in the HF, since it is positive definite.

Figure 2 provides a representation of the survival functions $s_W(a, b)$ and $s_H(a, b)$. We chose to illustrate these curves as a function of b , where a particular value of a is represented by an individual curve. Notably, for a positive-definite function such as the HF, all curves are monotonically decaying as a function

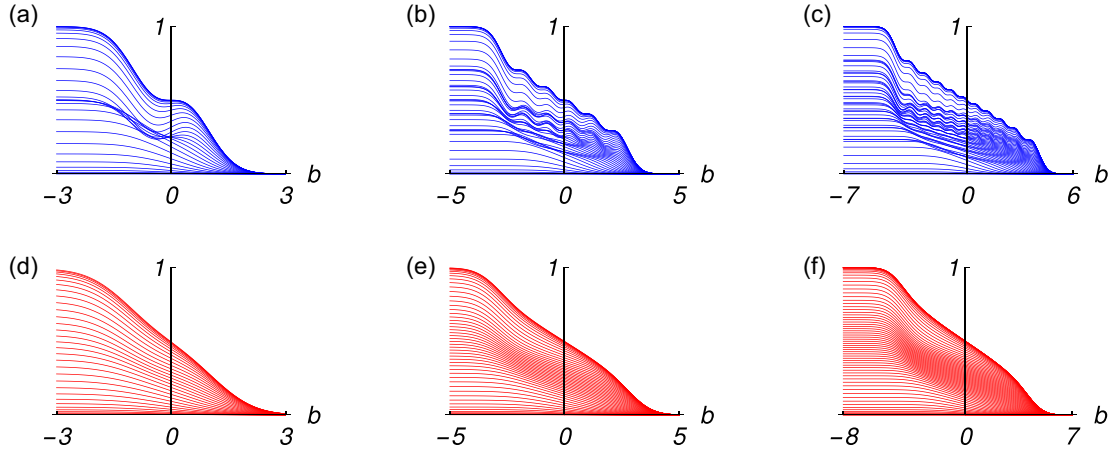


FIG. 2. Plots for (a)–(c) the survival function of the Wigner function $s_W(a, b)$ and (d)–(f) the survival function of the Husimi function $s_H(a, b)$ for states with (a) and (d) $n = 1$, (b) and (e) $n = 5$, and (c) and (f) $n = 10$. The plots are shown as a function of b , with each individual curve corresponding to a value of a in the interval $[-3, 3]$, $[-5, 5]$, $[-7, 6]$, and $[-8, 7]$ in steps of 0.2 units. Survival functions are dimensionless.

of either a or b . On the other hand, there are structures present in the curves corresponding to the WF, due to the presence of the negative regions. One can appreciate that these curves are not monotonically decreasing.

The WF and HF marginal densities can be compared in Fig. 3. Note that only position space marginal densities are presented, since for $\omega = 1$, $\rho(x) = \pi(p)$ and $\rho_H(x) = \pi_H(p)$. One can observe how the nodal structure increases with n for the position space density (WF marginal). On the other hand, this nodal structure is absent, or a broad average, in the HF marginal.

Figure 4 shows the WF and HF one-variable survival functions. First, the nodal structure in the position density translates into wiggles in the corresponding survival function [60]. In fact, there are $2n$ wiggles for each quantum state. The wiggles present in the WF survival functions are not present in those for the HF, since the HF marginal itself does not contain the nodal structure to the same extent as the WF.

B. Entropies of marginal distributions

We now present a discussion of the WF and HF marginal distribution entropies, before moving on to consider the WF and HF entropies. This is done since all marginal distributions are positive definite and there are no issues with complex-valued entropies. This provides a clearer comparison of the different entropic quantities and also allows a consideration of the differences between the WF and HF marginals. Establishing such a basis will allow for easier consideration of the interpretations, when the entropies of the WF and HF are discussed. Larger values of these entropies are associated with a delocalization of the underlying distribution.

Figure 5 presents the behavior of the Shannon entropy, the cumulative residual entropy, and the Rényi entropy for both the WF and the HF marginals with quantum number n . All entropic measures, using either the WF or HF marginals, increase with n . The important point is that the entropy of the WF marginal is always lower than the corresponding HF one, for a particular n . This observation is independent of

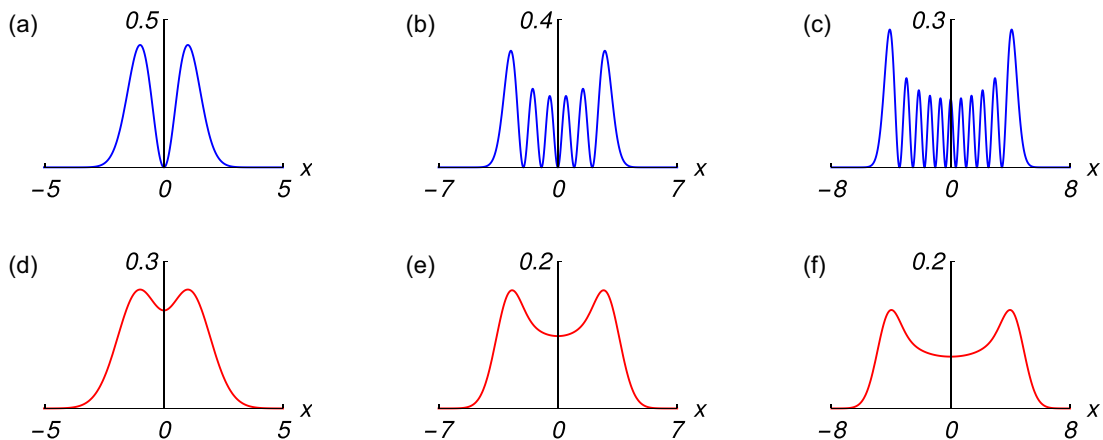


FIG. 3. Plots of (a)–(c) the Wigner function marginal densities $\rho(x)$ and (d)–(f) the Husimi function marginal densities $\rho_H(x)$ for states with (a) and (d) $n = 1$, (b) and (e) $n = 5$, and (c) and (f) $n = 10$. Densities are given in atomic units.

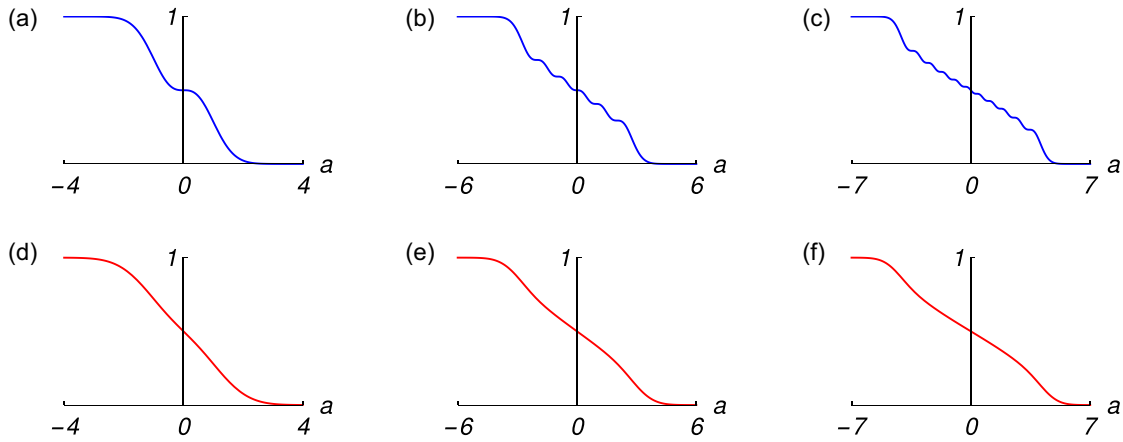


FIG. 4. Plots of (a)–(c) the survival functions for the Wigner function marginals $s_W^x(a)$ (d)–(f) the survival functions for the Husimi function marginals $s_H^x(a)$ for states with (a) and (d) $n = 1$, (b) and (e) $n = 5$, and (c) and (f) $n = 10$. Survival functions are dimensionless.

the entropic measure. Thus, the nodal structure present in the position space density (Figs. 3 and 4) yields that this density is more localized (smaller values) compared to the HF marginal. It is the loss of structure in the HF marginal compared to the WF one that is responsible for the higher entropic values of the HF marginals.

One could also ask how much the WF marginals resemble the HF ones and how this depends on n . The distance measures in Eqs. (16), (27), and (40) can be used to quantify this similarity or dissimilarity. This information is provided in Fig. 6. One can see that the interpretations from the first two measures are different. The S_{KL} measure illustrates that the distance between the position space density and the HF marginal (shown in Fig. 3) increases with n , while the R measure decreases with n . This is an important difference when considering the marginals or their survivals. This contrast can be explained by examining Figs. 3 and 4, where the marginals and the cumulative densities of HF and WF are shown. In Fig. 3 it is apparent that the difference between the distributions increases with n . The absence of structure in the HF marginals contrasts with the increasing number of nodes in the density (WF marginal). This is captured by S_{KL} in its increasing tendency as n increases. On the other hand, Fig. 4 shows that the nodes translate into wiggles in the survival distribution of the WF marginals, but they are less pronounced with increasing quantum number. Hence, for larger n , the cumulative distributions of the marginals seem to be more similar, as captured by R . The Rényi divergence D_R

is also presented. The increasing behavior is consistent with that of S_{KL} .

C. Entropies of the Wigner and Husimi functions

The preceding section established that the entropies of WF marginals are smaller than those of the corresponding HF marginals, due to the nodal structure that is present in the WF marginals. This is independent of the entropic definitions that are employed.

We now move on to examine the entropies of the Wigner and Husimi functions. The behaviors of the absolute value and the real component are shown in Fig. 7.

The Shannon entropy of the WF is complex valued for $n > 0$. For $n = 0$, the Wigner function is separable and is a product of the position and momentum space densities. Thus, its Shannon entropy is real valued for $n = 0$, while it is complex valued for $n > 0$. This can be seen from consideration of the real component and the absolute value. They are equal in the ground state, while they differ in the excited states. The Husimi function for the ground state ($n = 0$) is also separable into a product of its marginal densities. The HF Shannon entropies are real valued for all n , since the Husimi function is positive definite in ground and excited states.

An important point is that J is complex valued for $n > 0$, which illustrates that the auxiliary density defined in Eq. (30) as the integral over the WF has negative regions. On the other hand, one can observe that these regions must be smaller than those of the WF, since the real and absolute values almost

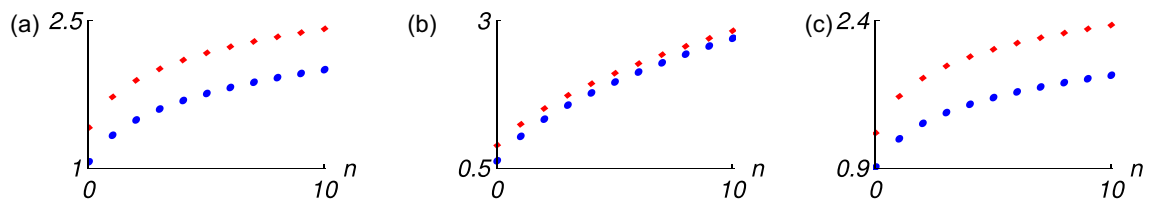


FIG. 5. (a) Plot of the Shannon entropies of the Wigner function marginal S_W^x (blue circles) and the Shannon entropies of the Husimi function marginal S_H^x (red diamonds) vs n . (b) Plot of the cumulative residual entropies of the Wigner function marginal C_W^x (blue circles) and the cumulative residual entropies of the Husimi function marginal C_H^x (red diamonds) vs n . (c) Plot of the Rényi entropies of the Wigner function marginal R_2^W (blue circles) and the Rényi entropies of the Husimi function marginal R_2^H (red diamonds) vs n . Units for all measures are in nat.

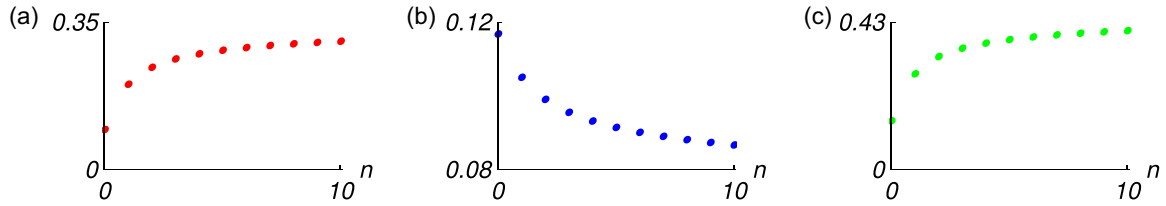


FIG. 6. (a) Kullback-Leibler distance S_{KL} (red circles) between the Wigner and Husimi marginals vs n . (b) Cumulative residual Jeffreys divergence R (blue circles) between the Wigner and Husimi marginals vs n . (c) Rényi divergence D_R (green circles) between the Wigner and Husimi marginals vs n . Units for all measures are in nat.

coincide in the J case. This is different from the Shannon entropy values, which illustrate a marked difference.

In addition, the interpretation from J is that the entropy of the WF is lower than that of the HF and increases with n . This is consistent with the observations from the marginal entropies. We now focus attention on the behavior of the Shannon entropy curves. If one considers the curve with the real component, it can be seen that its behavior is consistent with J ones, in that these values are lower than those of the corresponding HF ones. There is a crossover when considering the norm of the WF entropy and the HF entropy. This result for the absolute value here seems to be less appropriate when compared to the one for the real component.

Rényi entropies are shown in Fig. 8. Note that R_2^W is constant valued and does not depend on n . This contrasts with the R_2^H curve, which increases with n , and is consistent with the behavior observed for the other entropic measures. The R_4^W increases with n , which upon comparison to R_2^W illustrates the dependence of the Rényi entropy behavior on the parameter. The behaviors of R_4^W and R_4^H are consistent with the other measures in that they increase with n . Both the R_2^W and R_4^W values are lower than the corresponding R_2^H and R_4^H ones for a particular n . This relation between the WF and HF Rényi entropy values is consistent with that observed from the other entropic measures.

D. Entropic sums: Bounds and relations with phase-space entropies

We now discuss and compare the behavior of the entropic sums of the marginal distributions with those of the entropies

of the Wigner (real component) and Husimi distributions. These entropies and entropic sums are compared to the bounds given in Eqs. (18), (19), (26), and (39). Adjusted definitions are presented in Fig. 9 so that all quantities can be compared to the common bound $1 + \ln \pi$. The expressions are given in Table I. The absolute values of the Wigner function entropies are not shown since these were found to lie above the sum of the respective marginal entropies.

The distance to this bound, or uncertainty deficit, has been argued as the strength of a statement [35]. Stronger statements are associated with smaller distances. Note that the values of all quantities lie on the bound for the $n = 0$ state. Figure 9 illustrates that the phase-space entropies are all lower than the corresponding sum of the entropies of their marginals. While this is expected for S_H and the bound in Eq. (19), it also shows that the real components of the complex-valued entropies recover this tendency. This allows a conjecture on the presence of the real component of the corresponding WF entropies in Eqs. (18) and (26). The entropic sums of the WF marginals are also closer to the bound in comparison to the respective HF ones. The cumulative residual entropies present an exception to this behavior as the HF values are closer to the bound.

Most importantly, one observes that the real components of the WF entropies $\text{Re}(S_W)$ and $\text{Re}(J)$ are closer to the bound than the corresponding HF ones. The interpretation of this is that the WF entropies provide stronger statements than their HF counterparts.

The bounds for the Rényi entropies presented in Eqs. (39) and (44) are also obeyed. Another observation is that the

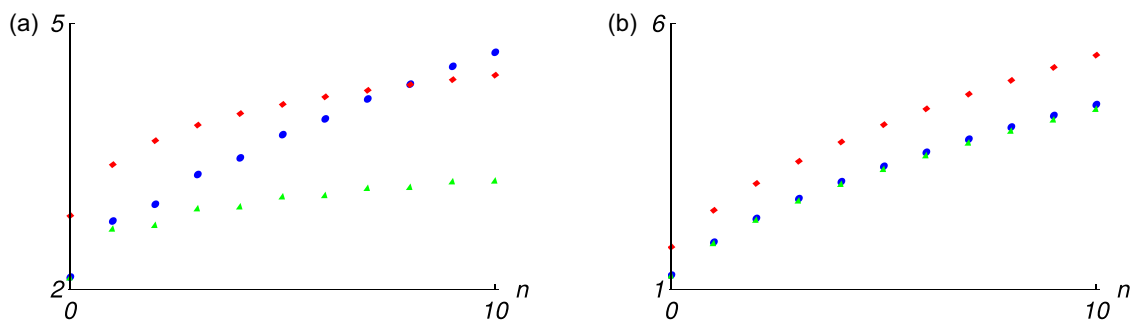


FIG. 7. (a) Plot of the absolute value of the Shannon entropy of the Wigner function $|S_W|$ (blue circles), the real part of the Shannon entropy of the Wigner function $\text{Re}(S_W)$ (green triangles), and the Shannon entropy of the Husimi function S_H (red diamonds) vs n . (b) Plot of the absolute value of the cumulative residual entropy of the Wigner function $|J_W|$ (blue circles), the real part of the cumulative residual entropy of the Wigner function $\text{Re}(J_W)$ (green triangles), and the cumulative residual entropy of the Husimi function J_H (red diamonds) vs n . Units for all measures are in nat.

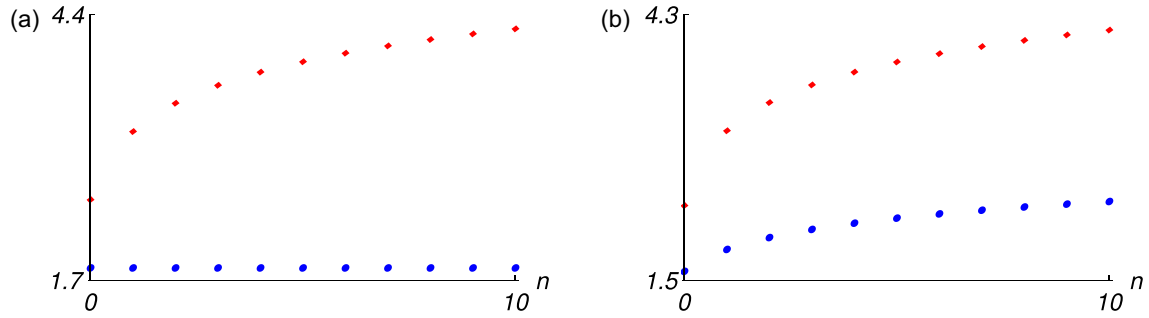


FIG. 8. Plots of the Rényi entropies of the Wigner function R_α^W (blue circles) and the Rényi entropies of the Husimi function R_α^H (red diamonds) with (a) $\alpha = 2$ and (b) $\alpha = 4$ vs n . Units for all measures are in nat.

Rényi entropy R_2^W sits on the bound and is the closest of all the measures. This contrasts with the behavior of R_4^H , which is farther away from the bound. It is noteworthy that both Rényi entropies of the WF are closer to the bound than the corresponding HF ones. Moreover, all phase-space Rényi entropies are closer to the bound compared to their corresponding entropic sums.

E. Correlation measures

The differences between the entropies of the phase-space distributions and those of the marginals were discussed in the preceding section. These differences can be quantified by examining the correlation measures. Larger values of these

measures imply a greater statistical correlation between the x and p variables.

The trends in the correlation measures with n are presented in Fig. 10. All correlation measures are zero valued for the $n = 0$ ground state. This is true for both the WF and HF measures, as these distributions are separable into a product of their respective marginals. The x - p correlation increases with n and is higher for the WF compared to the HF. In general, this is independent of the use of real components, or absolute values, in the mutual information and \mathcal{C} measures.

One should notice that the real part of the Wigner function mutual information yields an extremely small negative value (-0.01) for the $n = 1$ state. It is positive and increasing for

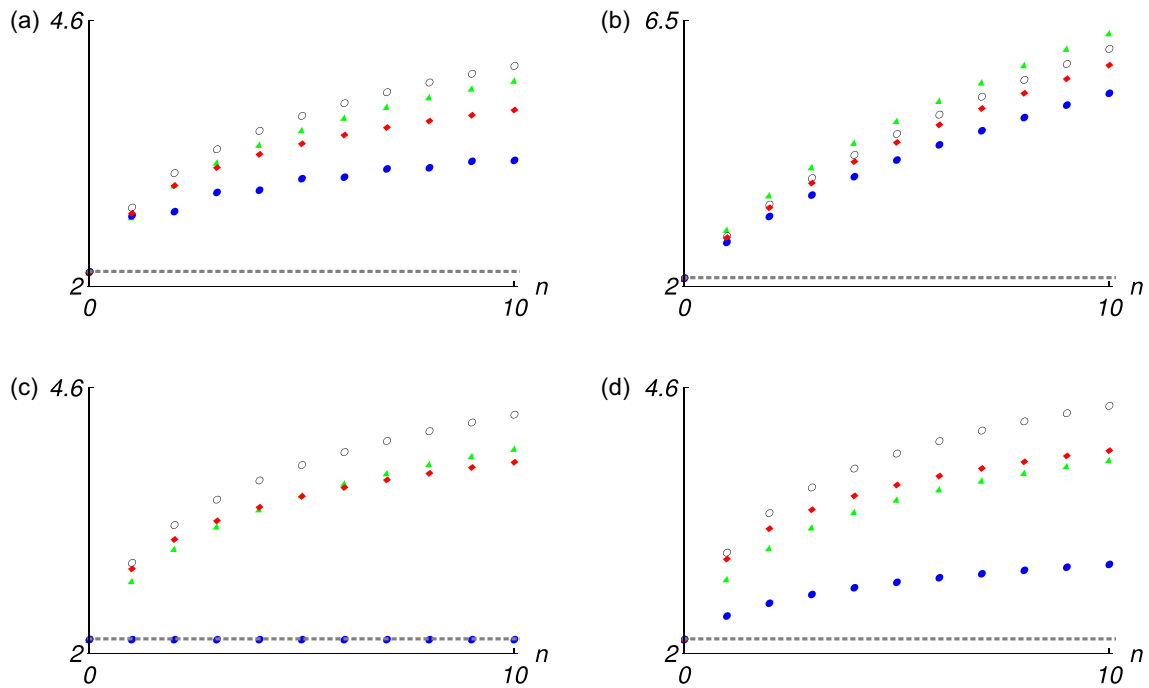


FIG. 9. Plots of (a) Shannon-like measures, (b) cumulative residual-like measures, and (c) and (d) Rényi-like measures vs n : (a) $S_H - \ln 2$ (red diamonds), $S_i(H) - \ln 2$ (black open circles), S_i (green triangles), and $\text{Re}(S_W)$ (blue closed circles); (b) $J_H - c_2 + 1 + \ln \pi$ (red diamonds), $S_i(C_H) - c_2 + 1 + \ln \pi$ (black open circles), $S_i(C_W) - c_1 + 1 + \ln \pi$ (green triangles), and $\text{Re}(J_W) - c_1 + 1 + \ln \pi$ (blue closed circles); (c) $R_2^H + 1 - \ln(4)$ (red diamonds), $S_i(R_2^H) + 1 - \ln(4)$ (black open circles), $S_i(R_2^W) + 1 - \ln(2)$ (green triangles), and $R_2^W + 1 - \ln(2)$ (blue closed circles); and (d) $R_4^H + 1 - \ln(2^{\sqrt[3]{4}})$ (red diamonds), $S_i(R_4^H) + 1 - \ln(2^{\sqrt[3]{4}})$ (black open circles), $S_i(R_4^W) + 1 - \ln(\sqrt[3]{4})$ (green triangles), and $R_4^W + 1 - \ln(\sqrt[3]{4})$ (blue closed circle). The horizontal line is the $1 + \ln \pi$ bound. Units for all measures are in nat.

TABLE I. Expressions used to evaluate the $1 + \ln \pi$ bound.

Shannon-like	Cumulative residual-like	Rényi-like
$S_H - \ln 2$	$J_H - c_2 + 1 + \ln \pi$	$R_2^H + 1 - \ln(4)$ $R_4^H + 1 - \ln(2\sqrt[3]{4})$
$S_t(H) - \ln 2$	$S_t(C_H) - c_2 + 1 + \ln \pi$	$S_t(R_2^H) + 1 - \ln(4)$ $S_t(R_4^H) + 1 - \ln(2\sqrt[3]{4})$
S_t	$S_t(C_W) - c_1 + 1 + \ln \pi$	$S_t(R_2^W) + 1 - \ln(2)$ $S_t(R_4^W) + 1 - \ln(\sqrt[3]{4})$
$\text{Re}(S_W)$	$\text{Re}(J_W) - c_1 + 1 + \ln \pi$	$R_2^W + 1 - \ln(2)$ $R_4^W + 1 - \ln(\sqrt[3]{4})$

the other states where $n > 1$. The I_{CS} measure, which is real valued, provides more evidence of the consistent behavior observed among all the measures. The Rényi mutual information of the HF is also shown in Fig. 10. Its behavior with n is consistent with the other correlation measures for the HF. The plot for the Rényi mutual information of the WF is not presented, since the integral that defines the measure diverges for $n > 0$. For $n = 0$, it is zero valued.

Figure 11 illustrates how the magnitude of the imaginary component increases negatively with n in the Wigner function mutual information and \mathcal{C} . Furthermore, Eqs. (17) and (31) show that these magnitudes of the imaginary components in the correlation measures are the negative of those in S_W and C_W , respectively. Thus, the volume of the negative regions in the Wigner function, which is proportional to these quantities, must increase with n .

IX. CONCLUSION

We compared and analyzed the behavior of various information-theoretic quantities when applied to Husimi and Wigner phase-space distributions. The former is positive definite while the latter is not. The question of the use of the Wigner function in an information-theoretic framework was addressed. This work also examined available options of formulating the entropic uncertainty relations in terms of phase-space distributions. The negative regions in Wigner functions yield Shannon and cumulative entropies with

imaginary components. The absolute value and real parts of these entropies increase with quantum number and are lower than the corresponding real-valued Husimi entropies. This relation is consistent with the results presented for the marginal entropies. On the other hand, there is a difference in behavior between the Rényi entropies ($\alpha = 2$) of the Wigner and Husimi functions. The Wigner function Rényi entropy is constant, while the Husimi function Rényi entropy increases with n . This changes when the Rényi entropy ($\alpha = 4$) parameter is altered. Both Wigner and Husimi Rényi entropies now increase with n , in accordance with the tendencies observed for the other entropies. The entropic sums of both the Wigner and Husimi function marginal densities and the corresponding phase-space entropies were examined with regard to the uncertainty relation bound. The real components of the Wigner function entropies were observed to be closer to the bound than the corresponding Husimi function ones. They were also closer to the bound than the respective entropic sums. These results are also consistent with those from the real-valued Rényi entropies. In fact, the Wigner function Rényi entropy with $\alpha = 2$ lies on the bound for all quantum numbers. Mutual information-type statistical correlation measures, which quantify the position-momentum correlation in the Wigner and Husimi functions, were also examined. These were observed to increase with n , with the interpretation that the correlation from the Wigner function is larger than the corresponding Husimi function one. Strikingly, both the absolute values and real components of the complex-valued

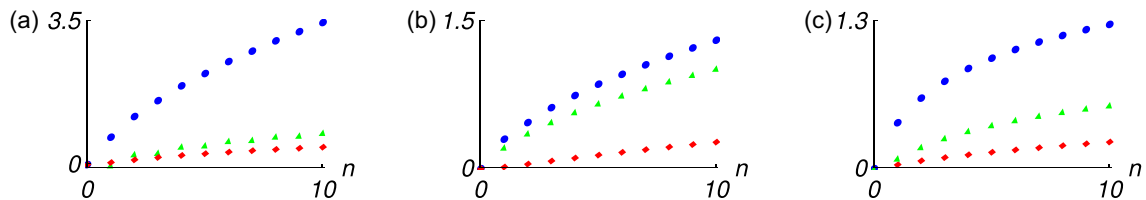


FIG. 10. (a) Plot of the absolute value of the Wigner function mutual information $|I_W|$ (blue circles), the real part of the Wigner function mutual information $\text{Re}(I_W)$ (green triangles), and the Husimi function mutual information I_H (red diamonds) vs n . (b) Plot of the absolute value of Wigner function cross cumulative residual entropy $|C_W|$ (blue circles), the real part of the Wigner function cross cumulative residual entropy $\text{Re}(C_W)$ (green triangles), and the Husimi function cross cumulative residual entropy C_H (red diamonds) vs n . (c) Plot of the Wigner function Cauchy-Schwarz information I_W^{CS} (blue circles) and the Husimi function Cauchy-Schwarz information I_H^{CS} (red diamonds) vs n and the Husimi function Rényi mutual information I_R^H (green triangles), with $\alpha = 2$ vs n . Units for all measures are in nat.

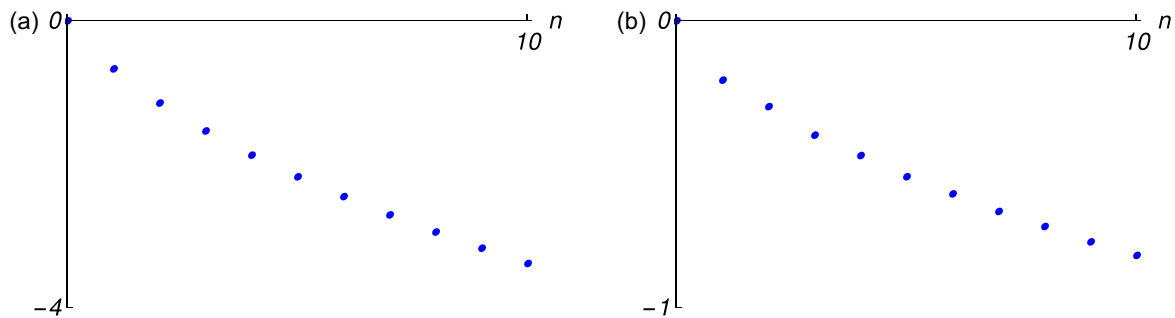


FIG. 11. Plots of (a) the imaginary component of the Wigner function mutual information $\text{Im}(I_W)$ and (b) the Wigner function cross-cumulative residual entropy $\text{Im}(C_W)$ vs n . Units for all measures are in nat.

Wigner measures displayed a tendency similar to the real-valued Cauchy-Schwarz mutual information of the Wigner function.

ACKNOWLEDGMENT

S.J.C.S. would like to thank CONACyT for a graduate fellowship.

- [1] S. R. Gadre, S. B. Sears, S. J. Chakravorty, and R. D. Bendale, Some novel characteristics of atomic information entropies, *Phys. Rev. A* **32**, 2602 (1985).
- [2] A. Grassi, G. M. Lombardo, N. H. March, and R. Pucci, $1/Z$ expansion, correlation energy, and Shannon entropy of heavy atoms in nonrelativistic limit, *Int. J. Quantum Chem.* **69**, 721 (1998).
- [3] P. Fuentealba and J. Melin, Atomic spin-density polarization index and atomic spin-density information entropy distance, *Int. J. Quantum Chem.* **90**, 334 (2002).
- [4] Q. Shi and S. Kais, Finite size scaling for the atomic Shannon information entropy, *J. Chem. Phys.* **121**, 5611 (2004).
- [5] R. Atre, A. Kumar, C. N. Kumar, and P. K. Panigrahi, Quantum information entropies of the eigenstates and the coherent state of the Pöschl-Teller potential, *Phys. Rev. A* **69**, 052107 (2004).
- [6] K. D. Sen, Characteristic features of Shannon information entropy of confined atoms, *J. Chem. Phys.* **123**, 074110 (2005).
- [7] K. C. Chatzisavvas, C. C. Moustakidis, and C. P. Panos, Information entropy, information distances, and complexity in atoms, *J. Chem. Phys.* **123**, 174111 (2005).
- [8] Á. Nagy, Shannon entropy density as a descriptor of Coulomb systems, *Chem. Phys. Lett.* **556**, 355 (2013).
- [9] G. H. Sun, S. H. Dong, and N. Saad, Quantum information entropies for an asymmetric trigonometric Rosen-Morse potential, *Ann. Phys. (Berlin)* **525**, 934 (2013).
- [10] A. J. Fotue, S. C. Kenfack, M. Tiotsup, N. Isofa, A. V. Wirngo, M. P. T. Djemmo, H. Fotsin, and L. C. Fai, Shannon entropy and decoherence of bound magnetopolaron in a modified cylindrical quantum dot, *Mod. Phys. Lett. B* **29**, 1550241 (2015).
- [11] C. H. Lin and Y. K. Ho, Shannon information entropy in position space for two-electron atomic systems, *Chem. Phys. Lett.* **633**, 261 (2015).
- [12] L. Delle Site, Shannon entropy and many-electron correlations: Theoretical concepts, numerical results, and Collins conjecture, *Int. J. Quantum Chem.* **115**, 1396 (2015).
- [13] S. A. Najafzade, H. Hassanabadi, and S. Zarrinkamar, Non-relativistic Shannon information entropy for Kratzer potential, *Chin. Phys. B* **25**, 040301 (2016).
- [14] A. Ghosal, N. Mukherjee, and A. K. Roy, Information entropic measures of a quantum harmonic oscillator in symmetric and asymmetric confinement within an impenetrable box, *Ann. Phys. (Berlin)* **528**, 796 (2016).
- [15] W. S. Nascimento and F. V. Prudente, Shannon entropy: A study of confined hydrogenic-like atoms, *Chem. Phys. Lett.* **691**, 401 (2018).
- [16] I. Nasser and A. Abdel-Hady, Fisher information and Shannon entropy calculations for two-electron systems, *Can. J. Phys.* **98**, 784 (2020).
- [17] C. O. Edet and A. N. Ikot, Shannon information entropy in the presence of magnetic and Aharonov-Bohm (AB) fields, *Eur. Phys. J. Plus* **136**, 432 (2021).
- [18] E. Cruz, N. Aquino, and V. Prasad, Localization-delocalization of a particle in a quantum corral in presence of a constant magnetic field, *Eur. Phys. J. D* **75**, 1434 (2021).
- [19] S. Bera, S. K. Haldar, B. Chakrabarti, A. Trombettoni, and V. K. B. Kota, Relaxation of Shannon entropy for trapped interacting bosons with dipolar interactions, *Eur. Phys. J. D* **74**, 73 (2020).
- [20] E. Romera and A. Nagy, Rényi information of atoms, *Phys. Lett. A* **372**, 4918 (2008).
- [21] J. Antolín, S. López-Rosa, and J. C. Angulo, Rényi complexities and information planes: Atomic structure in conjugated spaces, *Chem. Phys. Lett.* **474**, 233 (2009).
- [22] C. Martínez-Flores, M. Zeama, and I. Nasser, Shannon, Rényi entropies, and Fisher information calculations of the Li^{1+} and Be^{2+} ions screened by the ion-sphere plasma model, *Phys. Scr.* **96**, 065404 (2021).
- [23] N. Linden, M. Mosonyi, and A. Winter, The structure of Rényi entropic inequalities, *Proc. R. Soc. A* **469**, 0737 (2013).
- [24] P. Sánchez-Moreno, S. Zozor, and J. S. Dehesa, Upper bounds on Shannon and Rényi entropies for central potentials, *J. Math. Phys.* **52**, 022105 (2011).
- [25] J.-H. Ou and Y. K. Ho, Shannon, Rényi, Tsallis entropies and Onicescu information energy for low-lying singly excited states of helium, *Atoms* **7**, 70 (2019).

- [26] I. Nasser, M. Zeama, and A. Abdel-Hady, The Rényi entropy, a comparative study for He-like atoms using the exponential-cosine screened Coulomb potential, *Results Phys.* **7**, 3892 (2017).
- [27] I. Białynicki-Birula and J. Mycielski, Uncertainty relations for information entropy in wave mechanics, *Commun. Math. Phys.* **44**, 129 (1975).
- [28] W. Beckner, Inequalities in Fourier analysis, *Ann. Math.* **102**, 159 (1975).
- [29] A. Hertz and N. J. Cerf, Continuous-variable entropic uncertainty relations, *J. Phys. A: Math. Theor.* **52**, 173001 (2019).
- [30] A. Wehrl, On the relation between classical and quantum-mechanical entropy, *Rep. Math. Phys.* **16**, 353 (1979).
- [31] M. Grabowski, Wehrl-Lieb's inequality for entropy and the uncertainty relation, *Rep. Math. Phys.* **20**, 153 (1984).
- [32] H. G. Laguna and R. P. Sagar, Shannon entropy of the Wigner function and position-momentum correlation in model systems, *Int. J. Quantum Inf.* **08**, 1089 (2010).
- [33] I. Hornyák and A. Nagy, Inequalities for phase-space Rényi entropies, *Int. J. Quantum Chem.* **112**, 1285 (2012).
- [34] Z. Van Herstraeten and N. J. Cerf, Quantum Wigner entropy, *Phys. Rev. A* **104**, 042211 (2021).
- [35] S. Floerchinger, T. Haas, and H. Müller-Groeling, Wehrl entropy, entropic uncertainty relations, and entanglement, *Phys. Rev. A* **103**, 062222 (2021).
- [36] Á. Nagy, Phase-space Rényi entropy, complexity and thermodynamic picture of density functional theory, *J. Math. Chem.* **61**, 296 (2023).
- [37] E. P. Wigner, On the quantum correction for thermodynamic equilibrium, *Phys. Rev.* **40**, 749 (1932).
- [38] J. E. Moyal, Quantum mechanics as a statistical theory, *Math. Proc. Cambridge Philos. Soc.* **45**, 99 (1949).
- [39] C. K. Zachos, D. B. Fairlie, and T. L. Curtright, *Quantum Mechanics in Phase Space: An Overview with Selected Papers* (World Scientific, Singapore, 2005).
- [40] D. Wallace, in *Quantum Foundations of Statistical Mechanics*, edited by D. Bedingham, O. Maroney, and C. Timpson (Oxford University Press, Oxford, in press), doi: 10.48550/arXiv.2104.11223.
- [41] M. te Vrugt, G. I. Tóth, and R. Wittkowski, Master equations for Wigner functions with spontaneous collapse and their relation to thermodynamic irreversibility, *J. Comput. Electron.* **20**, 2209 (2021).
- [42] K. E. Cahill and R. J. Glauber, Ordered expansions in boson amplitude operators, *Phys. Rev.* **177**, 1857 (1969).
- [43] K. E. Cahill and R. J. Glauber, Density operators and quasiprobability distributions, *Phys. Rev.* **177**, 1882 (1969).
- [44] U. Leonhardt, *Measuring the Quantum State of Light* (Cambridge University Press, New York, 1997).
- [45] L. Cohen and Y. I. Zaporovanny, Positive quantum joint distributions, *J. Math. Phys.* **21**, 794 (1980).
- [46] K. Husimi, Some formal properties of the density matrix, *Proc. Phys. Math. Soc. Jpn.* **22**, 264 (1940).
- [47] G. Noguez, A. Rauschenbeutel, S. Osnaghi, P. Bertet, M. Brune, J. M. Raimond, S. Haroche, L. G. Lutterbach, and L. Davidovich, Measurement of a negative value for the Wigner function of radiation, *Phys. Rev. A* **62**, 054101 (2000).
- [48] O. Landon-Cardinal, L. C.-G. Góvia, and A. A. Clerk, Quantitative Tomography for Continuous Variable Quantum Systems, *Phys. Rev. Lett.* **120**, 090501 (2018).
- [49] K. Y. Spasibko, M. V. Chekhova, and F. Y. Khalili, Experimental demonstration of negative-valued polarization quasiprobability distribution, *Phys. Rev. A* **96**, 023822 (2017).
- [50] P. Zapletal and R. Filip, Multi-copy quantifiers for single-photon states, *Sci. Rep.* **7**, 1484 (2017).
- [51] F.-R. Winkelmann, C. A. Weidner, G. Ramola, W. Alt, D. Meschede, and A. Alberti, Direct measurement of the Wigner function of atoms in an optical trap, *J. Phys. B* **55**, 194004 (2022).
- [52] C. Kurtsiefer, T. Pfau, and J. Mlynek, Measurement of the Wigner function of an ensemble of helium atoms, *Nature (London)* **386**, 150 (1997).
- [53] D. M. Lu, Superposition of photon subtraction and photon addition excited squeezed thermal state and its Wigner function, *Int. J. Theor. Phys.* **56**, 3514 (2017).
- [54] E. H. Allen, Negative probabilities and the uses of signed probability theory, *Philos. Sci.* **43**, 53 (1976).
- [55] J. Harriman, Some properties of the Husimi function, *J. Chem. Phys.* **88**, 6399 (1988).
- [56] H. Schmider, *Representations and Interpretations of the Electronic One-Particle Density Matrix* (Queen's University, Kingston, 1994).
- [57] E. Colomé, Z. Zhan, and X. Oriols, Comparing Wigner, Husimi and Bohmian distributions: Which one is a true probability distribution in phase space? *J. Comput. Electron.* **14**, 894 (2015).
- [58] L. E. Ballentine, *Quantum Mechanics a Modern Development* (World Scientific, London, 1998).
- [59] M. Rao, Y. Chen, B. C. Vemuri, and F. Wang, Cumulative residual entropy: A new measure of information, *IEEE Trans. Inf. Theory* **50**, 1220 (2004).
- [60] H. G. Laguna, S. J. C. Salazar, and R. P. Sagar, Entropic Kullback-Leibler type distance measures for quantum distributions, *Int. J. Quantum Chem.* **119**, e25984 (2019).
- [61] V. I. Tatarskiĭ, The Wigner representation of quantum mechanics, *Sov. Phys. Usp.* **26**, 311 (1983).
- [62] I. Białynicki-Birula, Formulation of the uncertainty relations in terms of the Rényi entropies, *Phys. Rev. A* **74**, 052101 (2006).
- [63] S. Zozor and C. Vignat, On classes of non-Gaussian asymptotic minimizers in entropic uncertainty principles, *Physica A* **375**, 499 (2007).
- [64] J. C. Principe, D. Xu, Q. Zhao, and J. W. Fisher, Learning from examples with information theoretic criteria, *J. VLSI Signal Process. Syst. Signal Image Video Technol.* **26**, 61 (2000).
- [65] L. B. Gonçalves and J. L. R. Macrini, Rényi entropy and Cauchy-Schwartz mutual information applied to MIFS-U variable selection algorithm: A comparative study, *Pesqui. Oper.* **31**, 499 (2011).